A Biologically Based Model of Growth and Senescence of Syrian Hamster Embryo (SHE) Cells after Exposure to Arsenic

Kai H. Liao,[1,2] Daniel L. Gustafson,[3] Michael H. Fox,[4] Laura S. Chubb,[1] Kenneth F. Reardon,[2] and Raymond S.H. Yang[1]

Quantitative and Computational Toxicology Group, Center for Environmental Toxicology and Technology, Departments of [1]Environmental Health, [2]Chemical and Bioresource Engineering, Colorado State University, Fort Collins, Colorado, USA; [3]Department of Pharmaceutical Sciences, School of Pharmacy, University of Colorado Health Sciences Center, Denver, Colorado, USA; [4]Radiological Health Sciences, Colorado State University, Fort Collins, Colorado, USA

We modified the two-stage Moolgavkar-Venzon-Knudson (MVK) model for use with Syrian hamster embryo (SHE) cell neoplastic progression. Five phenotypic stages are proposed in this model: Normal cells can either become senescent or mutate into immortal cells followed by anchorage-independent growth and tumorigenic stages. The growth of normal SHE cells was controlled by their division, death, and senescence rates, and all senescent cells were converted from normal cells. In this report, we tested the modeling of cell kinetics of the first two phenotypic stages against experimental data evaluating the effects of arsenic on SHE cells. We assessed cell division and death rates using flow cytometry and correlated cell division rates to the degree of confluence of cell cultures. The mean cell death rate was approximately equal to 1% of the average division rate. Arsenic did not induce immortalization or further mutations of SHE cells at concentrations of 2 μM and below, and chromium (3.6 μM) and lead (100 μM) had similar negative results. However, the growth of SHE cells was inhibited by 5.4 μM arsenic after a 2-day exposure, with cells becoming senescent after only 16 population doublings. In contrast, normal cells and cells exposed to lower arsenic concentrations grew normally for at least 30 population doublings. The biologically based model successfully predicted the growth of normal and arsenic-treated cells, as well as the senescence rates. Mechanisms responsible for inducing cellular senescence in SHE cells exposed to arsenic may help explain the apparent inability of arsenic to induce neoplasia in experimental animals. *Key words*: **Arsenic, cancer modeling, cell proliferation, senescence, Syrian hamster embryo cell.** *Environ Health Perspect* **109:1207–1213 (2001). [Online 21 November 2001]**
http://ehpnet1.niehs.nih.gov/docs/2001/109p1207-1213liao/abstract.html

In vitro cell culture offers the advantage that cells from different stages of transformation can be isolated for detailed studies. Therefore, *in vitro* systems are useful for measuring the parameters needed for biologically based dose–response modeling. An *in vitro* system that has been used widely to assess the carcinogenic potential of chemicals is the Syrian hamster embryo (SHE) cell transformation system (*1,2*). Three important advantages of the SHE cell transformation system are that the cells exhibit a low frequency of spontaneous transformation; they readily demonstrate neoplastic transformation upon treatment with chemical carcinogens (*1*); and there exists a large database (*2–4*) on the carcinogenic potentials of chemicals.

We chose the two-stage Moolgavkar-Venzon-Knudson (MVK) model (*5–7*), which incorporates cell division, death, and mutation rates into the mechanistic description of malignant transformation, as the framework to describe the growth of SHE cells after exposure to chemical carcinogens. Cell division and death rates determine the population growth within each stage. Further, mutation likely occurs only at cell division.

The modified multistage carcinogenesis model for SHE cell neoplastic progression is shown in Figure 1. Normal cells in culture cease proliferation after a limited number of cell divisions, a process called cellular senescence. Escaping from senescence to become immortalized is the first important step during carcinogenesis in SHE cells and in many other cell types. Chemical carcinogens will, at some frequency, induce mutations in normal SHE cells that allow them an unlimited life span in culture. However, some chemical carcinogens, depending on the exposure concentrations, may inhibit the growth of SHE cells and shorten their life span instead of inducing immortal cell lines. Upon continued treatment with carcinogens, immortalized SHE cells will subsequently acquire additional mutations, some of which will confer the next important phenotypes—anchorage-independent growth and tumorigenic phenotypes. The verification of the conceptual model (Figure 1) and its five phenotypic stages require experiments involving different chemicals because no single chemical provides experimental results for all five phenotypic stages.

Based on the conceptual model presented in Figure 1, equations can be written to describe the time-dependent changes in the numbers of normal and senescent cells. We assume that the rate of change in the number of normal cells, dN(t)/dt, is proportional to the number of normal cells at any time:

$$\frac{dN(t)}{dt} = N(t) \times \left[\alpha(t) - \beta(t) - \gamma(t)\right] \quad [1]$$

In Equation 1, α and β represent the specific rates of cell division and death (units of reciprocal time) for normal cells, respectively, whereas γ is the specific rate at which normal cells convert to senescent cells (units of reciprocal time).

Similarly, the rate of change in the immortal cells, $dI(t)/dt$, has the same exponential growth property (with α_i and β_i being the specific rate of cell division and death, respectively), but there is also input of mutated normal cells:

$$\frac{dI(t)}{dt} = I(t) \times \left[\alpha_i(t) - \beta_i(t)\right] + \mu(t) \times \alpha(t) \times N(t) \quad [2]$$

The mutation rate, μ, is defined as the probability that a normal cell will divide into one normal cell and one immortal cell (immortality/cell division). The product of the mutation rate μ, the division rate α, and the number of normal cells describe the rate of change of the immortal cells caused by mutation.

The rate of change in the number of senescent cells, $dS(t)/dt$, is proportional to the specific senescence rate, γ, and the number of normal cells, because all senescent cells arise from normal cells:

$$\frac{dS(t)}{dt} = \gamma(t) \times N(t) \quad [3]$$

Address correspondence to R.S.H. Yang, Center for Environmental Toxicology and Technology, Colorado State University, Fort Collins, CO 80523 USA. Telephone: (970) 491-5652. Fax: (970) 491-8304. E-mail: Raymond.Yang@colostate.edu

This work was supported in part by a cooperative agreement with the Agency for Toxic Substances and Disease Registry (U61/ATU 881475), and National Institute for Environmental Health Sciences Superfund Basic Research Program Project (P42 ES05949) and research grant (RO1ES09655).

Received 24 October 2000; accepted 2 May 2001.

The goal of this work was to determine the rates of SHE cell division, death, senescence, and immortalization after exposure to arsenic, a known human carcinogen, and to evaluate the first stages of the modified multistage carcinogenesis model (Figure 1) for their ability to describe SHE cell growth dynamics. To obtain model predictions, we first determined values of the mutation rate μ, the division rate α, the death rate β, and the senescence rate γ by analyzing experimental data; we then used these values to simulate cell growth and senescence during four passages after exposure to a range of arsenic concentrations.

The justification for the modeling approach integrated with experimental verification is 3-fold: *a*) to work toward predictive capability, particularly when our conceptual model has been verified for all the phenotypic stages by a working set of chemicals; *b*) to incorporate more biologically relevant stages into the MVK model such that chemicals with carcinogenic activities at early or later stages may be identified and predicted on the basis of focused experiments using the SHE cell system; and *c*) to expand the SHE cell system to a more versatile short-term assay for carcinogenic potential of chemicals by integrating with computer modeling.

Materials and Methods

Cell culture. Golden Syrian hamsters (Charles Rivers Laboratories, Kingston, NY) at gestation day 13 were the sources of the primary embryo cells. The methods of establishing normal SHE cells were previously described by LeBoeuf et al. (*8,9*). Cell cultures were grown in Dulbecco's Modified Eagle's Medium-LeBoeuf's modification (Quality Biological Inc., Gaithersburg, MD) supplemented with 10% fetal bovine serum (Summit Biotechnology, Fort Collins, CO), 4 mM L-glutamine (Life Technologies, Grand Island, NY), 50 units/mL penicillin, and 50 μg/mL streptomycin (Life Technologies). Cells were incubated in humidified atmosphere with 10% CO_2 in air at 37°C.

Measurements of the life span of SHE cells. A vial of cryopreserved SHE cells was seeded in a T-150 flask and re-fed after 4 hr. After three days of incubation, cells were replated in 60-mm petri dishes at 4×10^4 cells per dish and incubated for 24 hr. Cells were then exposed to sodium *m*-arsenite for 2 days at four concentrations: 0.5, 1.0, 2.0, and 5.4 μM. The highest concentration, 5.4 μM, is the lethal concentration 50 (LC_{50}) of this chemical to SHE cells as determined by MTT (3-[4,5-dimethylthiazol-2-yl]-2,5-diphenyltetrazolium bromide; thiazol blue) assay. Parallel cell cultures were exposed to 3.6 μM chromium (a 1:1 mixture of chromium chloride hexahydrate and chromium oxide) and 100 μM of lead acetate trihydrate for 2 days. The four compounds used in the exposure experiments were purchased from Sigma Chemical Company (St. Louis, MO). We determined the life spans of SHE cells following serial passages. Cells were passaged once a week and replated at 4×10^4 cells in 4 mL of culture medium per 60-mm petri dish. Cell lines were determined to be senescent when they did not need to be passaged for more than 3 weeks and expressed cytoplasmic spreading.

Flow cytometry. We analyzed samples with an EPICS V cell sorter (Coulter, Miami, FL) interfaced to a Cicero data acquisition and display system (Cytomation, Inc., Fort Collins, CO). Cells were illuminated by an argon ion laser at 488 nm (500 mW). We used optical filters to measure fluorescein isothiocyanate (FITC) at wavelengths between 515 and 530 nm and propidium iodide (PI) at wavelengths longer than 610 nm. We used the software programs Multicycle and Multi2D (Phoenix Flow Systems, San Diego, CA) to analyze the univariate PI histograms and the bivariate bromodeoxyuridine/PI histograms.

Cell division rate measurement. We measured cell division rates using bromodeoxyuridine (BrdU; Sigma Chemical) incorporation with PI staining (Sigma Chemical), which allows calculation of potential doubling time (T_{pot}), a measure of cell cycle time that takes growth fraction but not cell loss into account (*10,11*). The relationship between T_{pot} and cell division rate (α) was defined as

$$\alpha = \frac{\ln 2}{T_{pot}} \qquad [4]$$

We measured potential doubling times with flow cytometry by pulse-labeling cells with BrdU and detecting its incorporation into DNA by the use of fluorescent antibodies. The cells were then counterstained by PI to measure the total DNA content.

The concept of potential doubling time was proposed by Steel (*10*). The calculation of potential doubling times using flow cytometric analysis results was later developed by Begg et al. (*12*). Briefly, the T_{pot} can be calculated as

$$T_{pot} = \lambda \times \frac{T_s}{LI}, \qquad [5]$$

where T_s is the period of DNA synthesis, *LI* (labeling index) is the fraction of cells synthesizing DNA, and λ is a correction factor for the nonlinear distribution of cells through the cell cycle (*10,11*). The labeling index is equal to the fraction of cells labeled by BrdU. We estimated the period of DNA synthesis (T_s) from the bivariate histogram of BrdU incorporation versus DNA content obtained by flow cytometry and the method of relative movement reported by Begg et al. (*12*).

The method for preparing BrdU-labeled cells was modified from Larsen (*13*). SHE cells were labeled by BrdU for 20 min and then fixed in 70% ethanol. To partially denature DNA, we incubated the cells in a solution of 0.2 mg pepsin in 1 mL 2N HCl at 37°C for 15 min. The cells were then incubated with monoclonal mouse anti-BrdU antibody (Dako, Carpinteria, CA) with a 1:27 dilution at room temperature for 30 min, followed by fluorescein isothiocyanate (FITC)-conjugated rabbit antimouse antibody (Dako) with 1:30 dilution for 15 min at room temperature. Finally, a solution

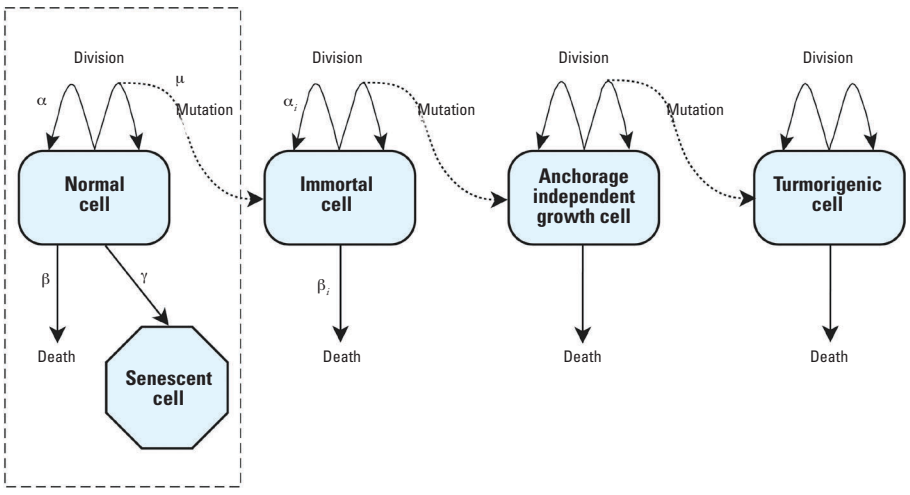

Figure 1. Conceptual model for SHE cell neoplastic progression. α and β are the cell division and death rates of normal cells, respectively. Similarly, α_i and β_i are the division and death rates of immortal cells. μ and γ are the mutation and senescence rates of normal cells. In this article we focus on the stages surrounded by the dashed line.

of 10 µg/mL of PI combined with 1 mg/mL of RNase (Sigma Chemical) was added to stain the DNA.

For division rate measurement, a gate on peak versus integral fluorescence of the PI signal was set to eliminate clumped cells. We analyzed 30,000 gated cells by flow cytometry for each sample.

Cell death rate measurement. We measured cell death rates in a time course study using a flow cytometric method based on PI staining specifically related to membrane damage. PI is taken up by dead cells only through the damaged membrane and is excluded by live cells (*14*). By setting a gate on forward angle light scatter (FALS), which is an indicator of cell size, we could partially exclude debris and clumps from flow cytometric measurement.

SHE cells were plated in parallel at 4×10^4 cells per dish. Samples were harvested at 72, 96, and 120 hr after plating. After all cells were collected, they were centrifuged and resuspended in 1 mL of 50 µg/mL PI and incubated at room temperature for 5 min; then 2×10^4 cells were analyzed by flow cytometry for each sample. Cells gated on FALS were examined on the basis of their uptake of PI, and the fraction of dead cells in the sample was obtained from these measurements.

Computer and software packages. The simulation programs were written in MATLAB (The MathWorks Inc., Natick, MA) and ACSL Tox (ACSL, Advanced Continuous Simulation Language; AEgis Technologies Group, Inc., Huntsville, AL) software packages and run on a Gateway P5-200 personal computer (Gateway, Inc., San Diego, CA). We used the Nelder-Mead simplex method to optimize model parameters.

Results

Estimation of mutation rates, µ. To estimate the mutation rate, we had first to determine the life span of SHE cells. SHE cells exposed to arsenic at 5.4 µM grew for only 16 population doublings before becoming senescent (Figure 2). The senescent cells were clearly distinct from normal cells in their morphology (cytoplasmic spreading) and very low culture growth rate. Furthermore, these cells were not dead; they remained attached and had intact membranes (as determined by Trypan Blue staining; data not shown). SHE cells exposed to lower concentrations (0.5, 1.0, or 2.0 µM) of arsenic grew for more than 30 population doublings and did not show significant differences in growth from control cells. We observed a similar lack of effect when SHE cells were exposed to chromium (3.6 µM) or lead (100 µM) (*15*).

We observed no cell immortalization under these arsenic exposure conditions, and thus the mutation rate, µ, was equal to the spontaneous immortalization rate of SHE cells. Bols et al. (*16*) reported that the spontaneous immortalization rate for SHE cells was calculated to be 6.1×10^{-10}/cell/generation as summarized from literature data. To be consistent with the units used in the model, the spontaneous immortalization rate was converted to 8.8×10^{-10} immortality/(cell division). This value is apparently an overestimate for our cell culture conditions because it suggests that cell immortalization should have been observed. Nevertheless, we used 8.8×10^{-10} immortality/(cell division) as the value of the mutation rate µ in the model.

Estimation of division rates, α. We used the potential doubling time (T_{pot}), determined by a flow cytometric method, to estimate the cell division rate, α (Equation 4). We observed in normal cells that T_{pot} was a function of time after each passaging of the cells (Figure 3). This effect was presumed to be a result of cell "crowding" on the petri dishes. Each passage began with the plating of 4×10^4 cells on each 60-mm petri dish. We observed low T_{pot} values (high cell division rates) while the cell density was low (Figure 4). As the cell density increased, longer T_{pot} values (low cell division rates) were measured, apparently due to decreased space for cells to grow (Figure 5). The result that the cell division rate is a function of "crowding" can be explained by the phenomenon of "density-dependent inhibition of cell division," which postulates that normal cells in culture stop dividing when a confluent monolayer is formed (*17*). Furthermore, a reduction of cell growth rates was detected when membrane contact occurred in a study conducted by video time-lapse microscopy in newborn rat dorsal root ganglion cells (*18*).

To incorporate the T_{pot} values measured into the model as the cell division rate, we used a nonlinear regression calculated by SigmaPlot to predict the relationship between T_{pot} (hour) and time after cells were passaged (hour),

$$T_{pot} = 12.4 + 0.0913 \times e^{0.0432 \times \text{time}} \quad [6]$$

This regression had a standard error of the estimate equal to 1.75 hr.

As cells approached senescence, they grew much more slowly than the normal cells (Figure 6). We observed T_{pot} values as high as 429 hr because only 2.3% of the cells were growing (LI = 0.023). The crowding factor did not play a major role in this case.

Estimation of death rates, β. The cell death rate (β) was constant within each passage and was defined as the value that provided the best fit of the following two equations to the experimental data for normal (N) and dead (D) cells:

$$\frac{dN(t)}{dt} = N(t) \times [\alpha(t) - \beta] \quad [7]$$

$$\frac{dD(t)}{dt} = N(t) \times \beta \quad [8]$$

A computer program was written in MATLAB to perform the linear regression required to obtain the death rate, β. The regression was achieved by using the Nelder-Mead simplex method to minimize objective function,

$$\textit{Objective Function} = \sum \left[\frac{(\textit{predicted} - \textit{observed})^2}{(\textit{observed})^{\omega}} \right], \quad [9]$$

where ω is the heteroscedasticity parameter. In this optimization, we used ω = 2 to represent relative weighting.

We calculated the mean cell death rate as $2.95 \times 10^{-4} \pm 0.64 \times 10^{-4}$ (hr^{-1}). This is approximately 1% of the average value of the

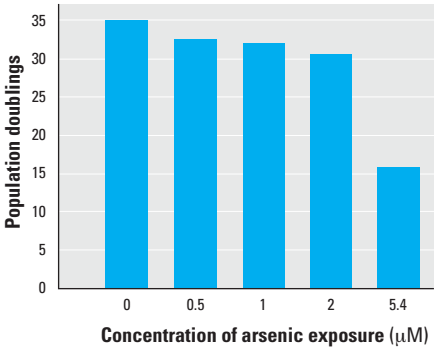

Figure 2. Effect of two-day arsenic exposure concentrations on the growth of SHE cells. Cell cultures exposed to 0, 0.5, 1.0, and 2.0 µM arsenic were still growing at the time the experiment was stopped.

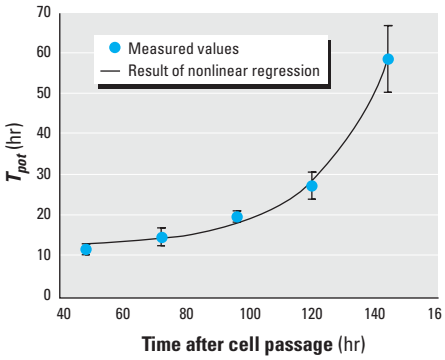

Figure 3. The change of SHE cell potential doubling time (T_{pot}) as a function of time after cell passage. Error bars indicate SD. The nonlinear regression is from the exponential equation $T_{pot} = 12.4 + 0.0913 \times e^{0.0432 \times \text{time}}$. SE of the estimate = 1.75 hr.

division rates. We observed no significant differences between the cell death rates of control and arsenic-treated cell lines.

Estimation of senescence rates, γ. The potential doubling times measured from the third and fourth passages of cells exposed to 5.4 μM of arsenic were much longer than those from the normal cells. From visual observation of the cells, we hypothesized that the increased potential doubling times of cells in these passages were caused by the increased fraction of senescent cells. In the following three sections, we first demonstrate the validity of this hypothesis, which also explains that cells exposed to 5.4 μM arsenic were becoming senescent during the third and fourth passages. Next, we derive the relationship between the senescence rate, γ, and the increased potential doubling time. Finally, we calculated the senescence rates by the potential doubling times measured from cells in the process of becoming senescent.

Demonstration of senescent cells causing the increases of potential doubling times. In a population containing both normal and senescent cells, the measured potential doubling times were affected by not only the "crowding" of cells on the petri dish, but also by the fraction of senescent cells. Thus, the more senescent cells in the population, the longer the T_{pot}. We determined the impact of the senescent cell populations on the T_{pot} values by normalizing the T_{pot} values by those measured at the third day after the cells were passaged (Figure 7). The normalized T_{pot} values provided information about the change of T_{pot} values within each passage, with all data presented

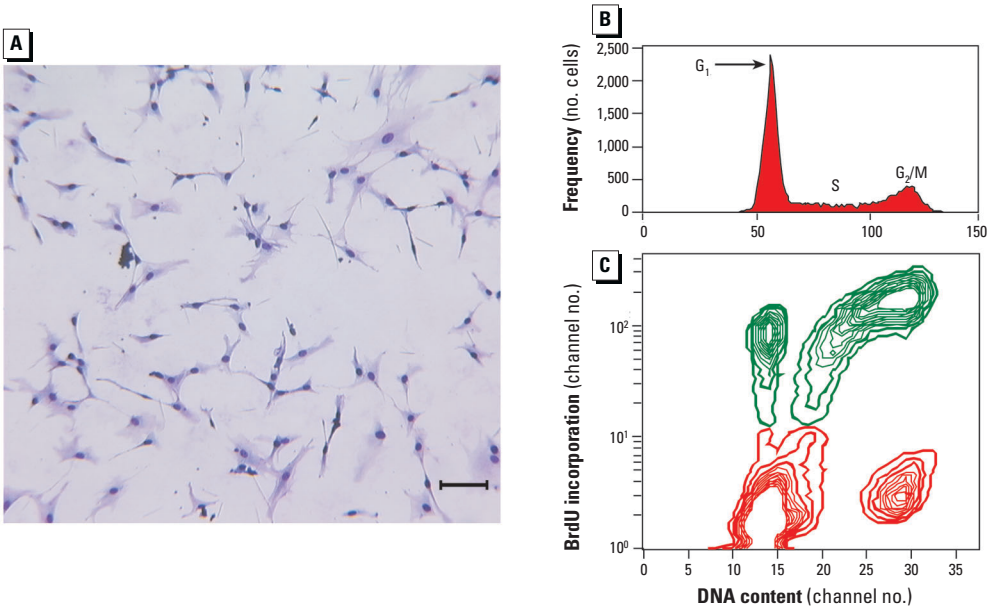

DNA synthesis time (T_s)	4.1 hr
Labeling index (LI)	0.32
Potential doubling time (T_{pot})	13 hr
Division rate (α)	0.053 hr^{-1}

Figure 4. The growth of normal SHE cells at low cell density (control cells at 72 hr after third passage). (*A*) Photomicrograph (bar = 100 μm). (*B*) Histograms from flow cytometric analysis represent the measurement of DNA content and (*C*) BrdU incorporation versus DNA content. (*D*) Parameters obtained from flow cytometric histogram analysis.

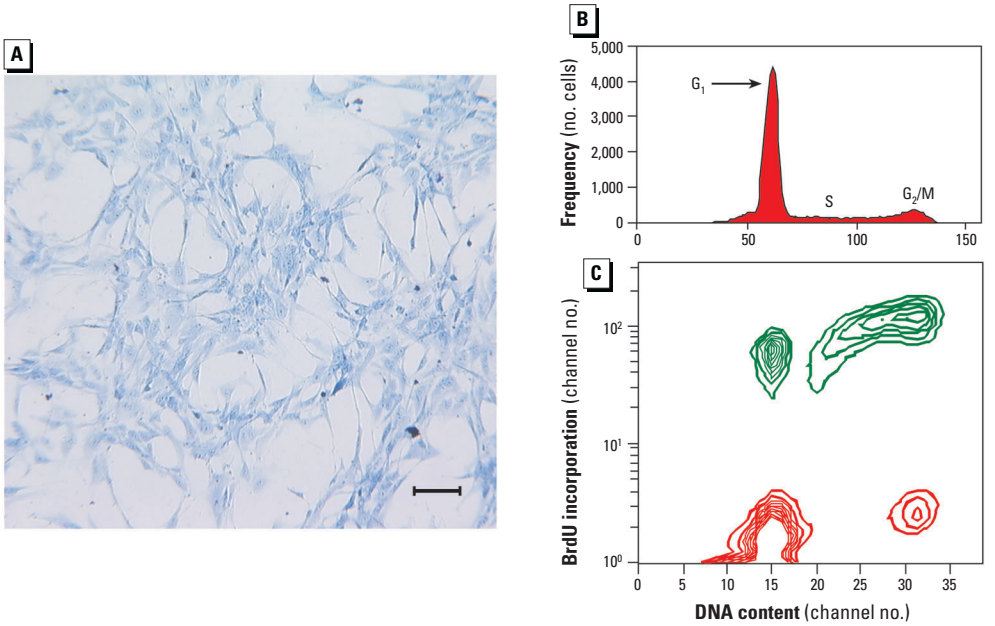

DNA synthesis time (T_s)	5.6 hr
Labeling index (LI)	0.248
Potential doubling time (T_{pot})	23 hr
Division rate (α)	0.030 hr^{-1}

Figure 5. The growth of normal SHE cells at high cell density (control cells at 120 hr after third passage). (*A*) Photomicrograph (bar = 100 μm). (*B*) Histograms from flow cytometric analysis represent the measurement of DNA content and (*C*) BrdU incorporation versus DNA content. (*D*) Parameters obtained from flow cytometric histogram analysis.

on a comparable scale. The standard curve represents the change of T_{pot} values caused only by the effect of crowding on normal cells (normalized from Equation 6). In all samples shown in Figure 7, T_{pot} values were measured only on the third and fifth days after cell passage.

The changes of the normalized T_{pot} values in control cells and cells exposed to the three lower concentrations of arsenic all followed the same pattern as standard curve, which suggests that their T_{pot} values were affected only by cell densities and not by senescence. For cells exposed to 5.4 µM arsenic, the normalized T_{pot} values increased 1.8- and 1.9-fold during the third and fourth passages over two days, but with only slight increases in the cell numbers. In contrast, the normalized T_{pot} values of the standard curve did not increase significantly with the same change in cell number. These results support the hypothesis that the senescent cells in the population lowered the labeling index and in turn caused the decreased growth rate of the whole population, i.e., the increased T_{pot} values. We can also conclude that cells exposed to 5.4 µM of arsenic were becoming senescent during the third and fourth passages.

The relationship between senescent cell numbers and potential doubling times. Because it is difficult to separate senescent cells from normal cells, we calculated the senescent cell numbers from the relationship between the measured potential doubling times and total cell numbers. The relationship is based on the phenomenon that the presence of senescent cells causes the decreased growth rate of the population. To distinguish the cell division rates measured in different populations, Equation 1 can be rewritten as

$$\frac{dN(t)}{dt} = N(t)\times[\alpha_{normal}(t)-\beta] - \gamma(t)\times N(t) \quad [10]$$

The normal cell division rate (α_{normal}) is the true cell division rate of normal cells, distinguished from the overall division rates that were actually measured at the third and fourth passages of the cells exposed to 5.4 µM of arsenic, α_{mix}, which is the division rate of a mixed population of normal and senescent cells. The relationship between α_{normal} and α_{mix} can be derived by first summing Equations 3 and 10:

$$\frac{d[N(t)+S(t)]}{dt} = N(t)\times\alpha_{normal}(t) - N(t)\times\beta \quad [11]$$

Because α_{mix} reflected the growth of the mixed population, which included the growing normal cells and nongrowing senescent cells, Equation 11 was rewritten as

$$\frac{d[N(t)+S(t)]}{dt} = [N(t)+S(t)] \times\alpha_{mix}(t) - N(t)\times\beta \quad [12]$$

Combining Equations 11 and 12, the fraction of normal cells in the mixed population was calculated as

$$\frac{N(t)}{N(t)+S(t)} = \frac{\alpha_{mix}(t)}{\alpha_{normal}(t)} \quad [13]$$

Using Equation 4, this can be rewritten as

$$\frac{N(t)}{N(t)+S(t)} = \frac{T_{pot,\ normal}(t)}{T_{pot,\ mix}(t)}, \quad [14]$$

where $T_{pot,\ normal}$ is the potential doubling time for normal cells and $T_{pot,\ mix}$ is the potential doubling time for a cell population containing normal and senescent cells. The ratio of senescent cells (S) to total cells (N+S) was then calculated by Equation 14.

Calculation of senescence rates. We estimated the senescence rates (γ) by optimizing the model fit to the estimated number of senescent cells (Equation 3) and normal cells (Equation 10). The predicted numbers of senescent cells were verified compared to values calculated from Equation 14 (based on experimental data), whereas the summation of predicted normal and senescent cells were verified by the data calculated from Equation 12. The crowding factor correction for the third and fourth passage of 5.4 µM-treated cells had to be modified because the senescent cells occupied much larger areas on the petri plates than did normal cells. By using the Nelder-Mead simplex method in an ACSL program, we optimized the numeric values of the correction factor and the senescence rates simultaneously to provide the best fit of the prediction of total and senescent cell numbers to the experimental data. The modified correction factor to the division rates of

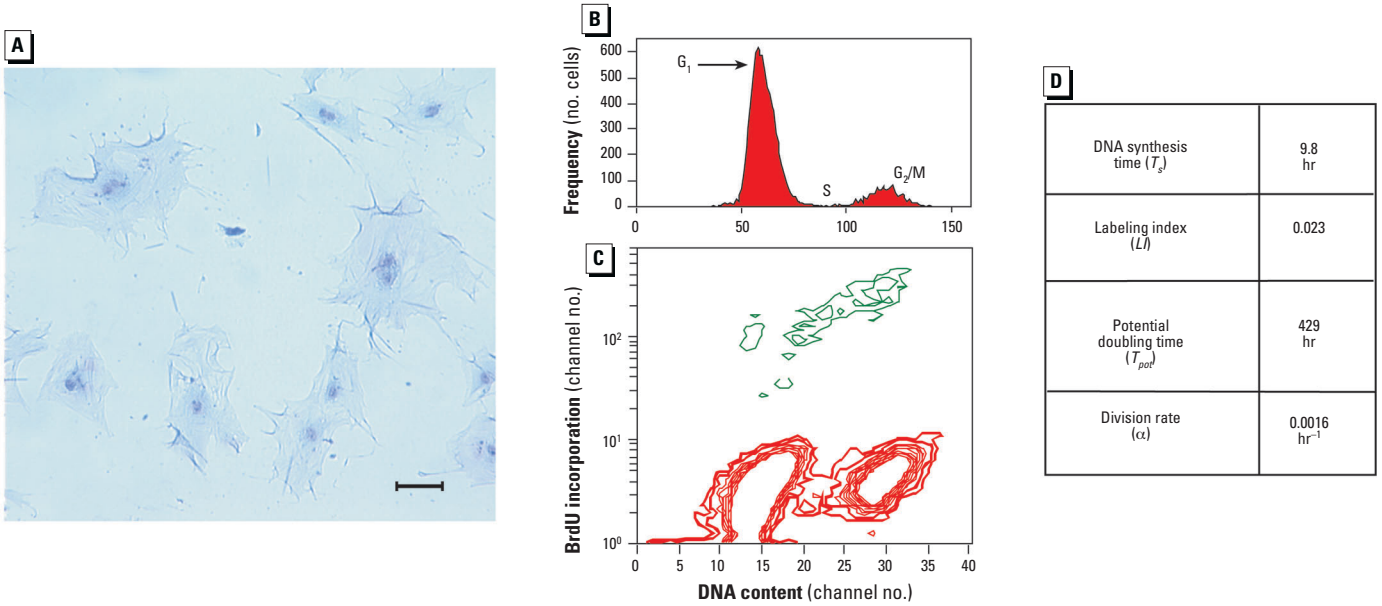

Figure 6. The growth of SHE cells when approaching cellular senescence (5.4 µM arsenic-treated cells at fourth passage). (*A*) Photomicrograph (bar = 100 µm). (*B*) Histograms from flow cytometric analysis represent the measurement of DNA content and (*C*) BrdU incorporation versus DNA content). (*D*) Parameters obtained from flow cytometric histogram analysis.

the normal cells was determined to be 0.37. The senescence rates were estimated as 0.0101 hr^{-1} for the third passage and 0.0175 hr^{-1} for the fourth passage with the corrected normal cell division rates. All the model parameters are summarized in Table 1.

Discussion

Effects of arsenic exposure. In these experiments, exposure to 5.4 µM arsenic led to senescence rather than immortalization. Although arsenic is a known human carcinogen (*19*), little evidence has been found for its carcinogenicity in animal models (*20*). However, Ng et al. (*21*) recently reported that tumors were observed in C57Bl/6J and metallothionein knock-out transgenic mice given sodium arsenate (500 µg As/L *ad libitum*) in drinking water for up to 26 months. Malignant tumors were also produced in Nude mice inoculated with a rat liver epithelial cell line (TRL 1215) after continuous *in vitro* exposure to sodium arsenite (0.125, 0.250, and 0.500 µM) for 18 weeks (*22*).

Cellular senescence induced by arsenic has not been previously reported. However, arsenic induced mitotic inhibition in Chinese hamster ovary cells (*23*), and induction of cellular senescence has also been reported with exposure to radiation (*24*). Furthermore, arsenic at certain concentrations caused inhibition, *in vivo*, of the promotion of preneoplastic lesions in rats (*25*) and decreased tumor incidence in mice (*26*), although the processes underlying these effects remain unknown. Mechanisms involved in the induction of cellular senescence by arsenic *in vitro* may be related to the effects observed *in vivo*.

Model prediction of the growth and senescence of SHE cells. To model SHE cell dynamics following lower arsenic exposures, we incorporated values of the experimentally determined cell division and death rates into Equation 1 as the basis for a model that we used to predict the total cell number. For this purpose, γ was taken to be zero—i.e., senescence was not considered. The model incorporated a lag phase, where the cell numbers remains unchanged; this is necessary to reflect the growth characteristics immediately after replating the cells. During this period, we observed little or no growth possibly because the cells adapted in a newly created cell culture environment. The model also included the observation that the growth rate slowed as the cell density increased (Figure 3). Thus, in the model prediction (Figure 8), there is a lag phase at the beginning of each passage, followed by a rapidly growing phase with low cell density. At higher density, cells grew at a lower rate. Cells were passaged weekly and another lag phase started at this point. The value of lag time (t_{lag}; 41.9 hr) was optimized using the Nelder-Mead simplex method in an MATLAB program based on experimental data.

The model prediction describes the growth of control cells and cells exposed to low arsenic concentrations well. The results in Figure 8 indicate that there was no significant difference in growth between control cells and the cell lines treated with three lower concentrations of arsenic, 0.5, 1.0, and 2.0 µM. The cell numbers in these four treatments all fell in the area represented by the uncertainty of the model, and agreed with the assumption that cells did not undergo senescence with these experimental conditions. The uncertainty of the model was estimated based on the T_{pot} standard error (1.75 hr). On the other hand, SHE cells exposed to 5.4 µM arsenic grew much more slowly in the third and fourth passages. This cell line stopped growing at the fourth passage. Clearly, senescence was an important factor in the growth of the SHE cell population and the inclusion of senescence rates was required. With senescence rates applied to the model, the total number of cells (sum of normal and senescent cells) were well predicted for cells in the process of becoming senescent, i.e., cells exposed to 5.4 µM arsenic at the third and fourth passages. (Figure 8).

With use of the estimated senescence rates, the numbers of normal and senescent cells separately were also predicted for cells becoming senescent (Figure 9). The simulation for senescent cells, though in agreement with the trend of the senescent cell numbers estimated from Equation 14, does not provide a good quantitative prediction. To improve further the estimation of senescence rates, an accurate method for monitoring the appearance of senescent cells is required.

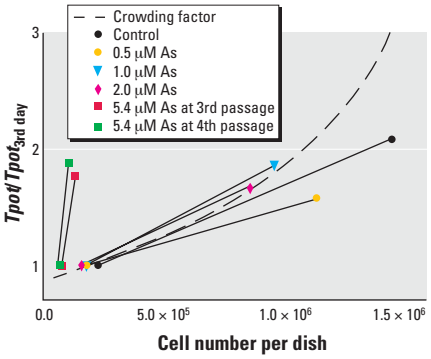

Figure 7. The effect of senescent cell population on potential doubling time (T_{pot}). Potential doubling times were normalized according to the value measured at the third day after the fourth passage in each cell line. Symbols represent normalized T_{pot} values.

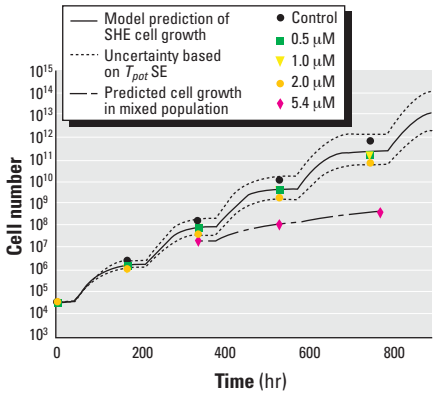

Figure 8. Model prediction of the growth of SHE cells. SE = 1.75 hr. Symbols represent corrected cell numbers of cells exposed to arsenic for 2 days.

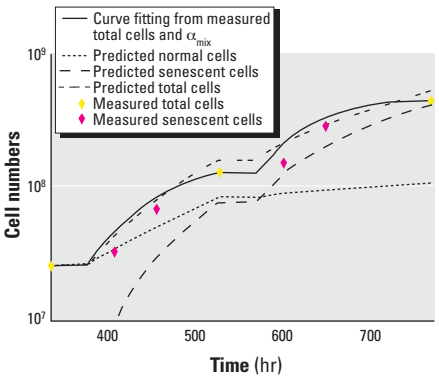

Figure 9. Comparison of predicted and measured cell types during the third and fourth passages of SHE cells exposed to 5.4 µM arsenic for 2 days.

Table 1. Model parameters.

	Division rate α (hr^{-1})[a]	Death rate β (hr^{-1})	Senescence rate γ (hr^{-1})	Mutation rate µ (immortality/ cell division)
Control and 0–2.0 µM As	$\ln 2/(12.4 + 0.0913 \times e^{0.0432 \times tp})$	2.95×10^{-4}	0	8.8×10^{-10}
5.4 µM As at 3rd passage	$0.37 \times (0.0544 - 3.63 \times 10^{-8} \times NS + 1.01 \times 10^{-14} \times NS^2 - 2.25 \times 10^{-21} \times NS^3)$	2.95×10^{-4}	0.0101	8.8×10^{-10}
5.4 µM As at 4th passage	$0.37 \times (0.0544 - 3.63 \times 10^{-8} \times NS + 1.01 \times 10^{-14} \times NS^2 - 2.25 \times 10^{-21} \times NS^3)$	2.95×10^{-4}	0.0175	8.8×10^{-10}

Abbreviations: NS, total number of cells in a 60-mm petri dish; tp, time after passage (hours).
α, β, and γ were determined experimentally; µ is taken from the literature. Because division rates were influenced by the density of cells on a plate, equations are required to represent α at different points in a cell passage.

Conclusions

Arsenic exposure has rarely been shown to be carcinogenic in animal models. On the other hand, our *in vitro* experiments demonstrated that exposure to arsenic induced senescence in SHE cells. A possible link between these observations is the hypothesis that mechanisms responsible for arsenic-induced senescence may be involved in the apparent inability of arsenic to induce neoplasia in experimental animals. In combination with an appropriate human *in vitro* system, the SHE cell system could serve as a tool for comparing differences in carcinogenic mechanisms of arsenic between laboratory animals and humans.

The biologically based dose–response model developed here successfully predicted the growth of normal and arsenic-treated SHE cells. Independent measurements of cell division and death rates, determined using flow cytometry, could be incorporated in the model to provide predictions that were consistent with the experimental data. The flow cytometric methods used here can be applied easily to other cell lines for modeling purposes.

This model of normal and senescent cell dynamics can be used for exposure to other chemicals and for other cell lines. Its development is the first phase of our overall goal of integrating cellular and mechanistic studies with computer modeling to develop a predictive tool for assessing carcinogenic potentials of chemical and chemical mixtures. Work in progress includes the addition of three more stages of neoplastic progression in this cell model—immortal, anchorage-independent growth and tumorigenic—as well as the related experimental and computer modeling studies.

References and Notes

1. Barrett JC. Neoplastic progression of Syrian hamster embryo cells in culture. Proc Soc Exp Biol Med 202:30–36 (1993).
2. Aardema MJ, Isfort RJ, Thompson ED, LeBoeuf RA. The low pH Syrian hamster embryo (SHE) cell transformation assay: a revitalized role in carcinogen prediction. Mutat Res 356:5–9 (1996).
3. LeBoeuf RA, Kerckaert GA, Aardema MJ, Gibson DP, Brauninger R, Isfort RJ. The pH 6.7 Syrian hamster embryo cell transformation assay for assessing the carcinogenic potential of chemicals. Mutat Res 356:85–127 (1996).
4. Isfort RJ, Kerckaert GA, LeBoeuf RA. Comparison of the standard and reduced pH Syrian hamster embryo (SHE) cell *in vitro* transformation assays in predicting the carcinogenic potential of chemicals. Mutat Res 356:11–63 (1996).
5. Moolgavkar SH. Two-event models for carcinogenesis: incidence curves for childhood and adult tumors. Math Biosci 47:55–77 (1979).
6. Moolgavkar SH, Knudson AG Jr. Mutation and cancer: a model for human carcinogenesis. J Natl Cancer Inst 66:1037–1052 (1981).
7. Moolgavkar SH, Dewanji A, Venzon DJ. A stochastic two-stage model for cancer risk assessment. I. The hazard function and the probability of tumor. Risk Anal 8:383–392 (1988).
8. LeBoeuf RA, Kerckaert GA, Poiley JA, Raineri R. An interlaboratory comparison of enhanced morphological transformation of Syrian hamster embryo cells cultured under conditions of reduced bicarbonate concentration and pH. Mutat Res 222:205–218 (1989).
9. LeBoeuf RA, Kerckaert GA. The induction of transformed-like morphology and enhanced growth in Syrian hamster embryo cells grown at acidic pH. Carcinogenesis 7:1431–1440 (1986).
10. Steel GG. Basic theory of growing cell populations. In: Growth Kinetics of Tumours: Cell Population Kinetics in Relation to the Growth and Treatment of Cancer (Steel GG, ed). Oxford:Clarendon Press, 1977;57–85.
11. Wilson GD. Analysis of DNA-measurement of cell kinetics by the bromodeoxyuridine/anti-bromodeoxyuridine method. In: Flow Cytometry: A Practical Approach (Ormerod MG, ed). Oxford:Oxford University Press, 1994;137–156.
12. Begg AC, McNally NJ, Shrieve DC, Karcher H. A method to measure the duration of DNA synthesis and the potential doubling time from a single sample. Cytometry 6:620–626 (1985).
13. Larsen JK. Measurement of cytoplasmic and nuclear antigens. In: Flow Cytometry: A Practical Approach (Ormerod MG, ed). Oxford:Oxford University Press, 1994;93–117.
14. Ormerod MG. Further applications to cell biology. In: Flow Cytometry: A Practical Approach (Ormerod MG, ed). Oxford:Oxford University Press, 1994;261–273.
15. Liao KH. Initial Development of A Multistage Cancer Model Based on Syrian Hamster Embryo (SHE) Cell Transformation Studies [M.S. Thesis]. Fort Collins, CO:Colorado State University, 1999.
16. Bols BLMC, Naaktgeboren JM, Simons JWIM. Immortalization of Syrian hamster embryo cells is in itself a multistep event. Cancer Res 51:1177–1184 (1991).
17. Alberts B, Bray D, Lewis J, Raff M, Roberts K, Watson JD. The cell-division cycle. In: Molecular Biology of the Cell New York:Garland Publishing, 1994;863–910.
18. Bandtlow C, Zachleder T, Schwab ME. Oligodendrocytes arrest neurite growth by contact inhibition. J Neurosci 10:3837–3848 (1990).
19. National Research Council: Subcommittee on Arsenic in Drinking Water. Arsenic in Drinking Water. Washington, DC:National Academy Press, 1999.
20. Barrett JC, Lamb PW, Wang TC, Lee TC. Mechanisms of arsenic-induced cell transformation. Biol Trace Elem Res 21:421–429 (1989).
21. Ng JC, Seawright AA, Qi L, Garnett CM, Chiswell B, Moore MR. Tumours in mice induced by exposure to sodium arsenate in drinking water. In: Arsenic Exposure and Health Effects (Chappel WR, Abernathy CO, Calderon RL, eds). Oxford:Elsevier Science, 1999;217–223.
22. Zhao CQ, Young MR, Diwan BA, Coogan TP. Association of arsenic-induced malignant transformation with DNA hypomethylation and aberrant gene expression. Proc Natl Acad Sci USA 94:10907–10912 (1997).
23. Lee TC, Lee KCC, Chang C, Jwo WL. Cell-cycle dependence of the cytotoxicity and clastogenicity of sodium arsenite in Chinese hamster ovary cells. Bull Inst Zool Acad Sin 25:91–97 (1986).
24. Peters LJ. Radiation therapy tolerance limits. For one or for all?—Janeway Lecture. Cancer 77:2379–2385 (1996).
25. Pott WA, Benjamin SA, Yang RSH. Antagonistic interactions of an arsenic-containing mixture in a multiple organ carcinogenicity bioassay. Cancer Lett 133:185–190 (1998).
26. Kanisawa M, Schroeder HA. Life term studies on the effects of arsenic, germanium, tin, vanadium on spontaneous tumors in mice. Cancer Res 27:1192–1195 (1967).